J. Korean Inst. Electr. Electron. Mater. Eng.
Vol. 38, No. 1, pp. 65-71 January 2025
doi: https://doi.org/10.4313/JKEM.2025.38.1.8
ISSN 1226-7945(Print), 2288-3258(Online)

Regular Paper

Influence of Al Content on the Resonant Characteristics of Al-Mo Thin Film-Based SAW Devices

Jae-Cheol Park

Purpose-Based Mobility Group, Korea Institute of Industrial Technology, Gwangju 61012, Korea

(Received September 20, 2024; Revised October 10, 2024; Accepted October 10, 2024)

Abstract: Al-Mo thin films were fabricated using combinatorial sputtering system to realize highly sensitive surface acoustic wave (SAW) devices. The Al-Mo sample library was grown with various chemical compositions and electrical resistivities, which provided important information for selecting the most suitable materials for SAW devices. As the SAWs generated from piezoelectric materials are significantly affected by the resistivity and density of the interdigital transducer (IDT) electrodes, three types of Al-Mo thin films with different Al contents were fabricated. The thickness of the Al-Mo thin film used in the SAW-IDT electrode was fixed at 150 nm. As the Al content of the Al-Mo thin film decreased from 81.2 to 30.3 at%, the resistivity decreased slightly from 5.43±0.15 to 4.87±0.1×10^{-5} Ω-cm, whereas the calculated density increased significantly from 4.1 to 7.9 g/cm^3. The SAW device composed of Al-Mo IDT electrodes resonated at 143 MHz without frequency shifts; however, the selectivity of the resonant frequency and insertion loss deteriorated as the Al content decreased. This suggest that the resonant characteristics of the SAW devices fabricated with Al-Mo thin films were more strongly influenced by the material density rather than the electrical properties of the IDT electrodes.

Keywords: Combinatorial sputtering, Surface acoustic wave, Interdigital transducer, Aluminum-molybdenum, Thin film

1. INTRODUCTION

Surface acoustic wave (SAW) sensors have gained widespread adoption across various industries due to their exceptional performance, high frequency, and low insertion loss [1-3]. A critical component of SAW sensors, the interdigital transducer (IDT), significantly influences the overall sensor performance. IDTs leverage the piezoelectric effect to convert electrical energy into mechanical vibrations. When a voltage is applied to the IDT electrodes, the inverse piezoelectric effect induces mechanical deformation, generating SAWs along the substrate surface [4,5]. These waves interact with adsorbed substances on the sensor's surface, causing a frequency shift that can be measured to detect external environmental changes. Traditionally, noble metals have been employed as IDT materials [6], but their high density could limit the generation of high-frequency SAWs, resulting in reduced sensor sensitivity and frequency response. While aluminum is suitable for generating high-frequency SAWs, its low electrical conductivity can lead to signal losses. To address these limitations, researchers have been exploring novel IDT materials with enhanced piezoelectric properties, lower density, and higher electrical conductivity.

This study investigates the utilization of physically mixed aluminum (Al) and molybdenum (Mo) composite films as IDT electrode materials for the SAW sensors. Al is a lightweight material with relatively good electrical properties, making it suitable for SAW applications. However, its susceptibility to oxidation at room temperature can lead to degradation of its

✉ **Jae-Cheol Park; jerwual@kitech.re.kr**

electrical performance. Mo, while having lower electrical conductivity than Al, exhibits stable electrical properties at high temperatures and offers excellent chemical and abrasion resistance, ensuring long-term stability of the SAW device electrodes. By combining Al and Mo into a composite film, we aim to leverage the complementary properties of each element, achieving a material with enhanced electrical conductivity, high-temperature stability, and corrosion resistance.

In this study, combinatorial sputtering [7-9] was employed to fabricate Al-Mo composite thin films consisting of physically mixed Al and Mo elements. This approach prevents the formation of the alloy, maximizing the advantages of each element. The Al-Mo phase diagram supports the formation of a stable composite at room temperature due to limited diffusion. This study aims to elucidate the influence of compositional variations in Al-Mo composite films on the resonant characteristics of SAW devices. By identifying the optimal composition, we aim to develop physically mixed Al-Mo composite thin films that enhance the performance of SAW sensors and enable stable operation in various environments.

2. EXPERIMENTAL DETAIL

Al-Mo thin films with varying chemical, structural, and electrical properties were grown on 4-inch silicon (Si) substrates using combinatorial RF sputtering (ULVAC MB07-4501). These films were then systematically investigated for their application as SAW-IDT electrodes. In an effort to fabricate the Al-Mo thin films, single metal Al and Mo targets were employed, and the films were grown in a fixed state without substrate rotation to establish a compositional gradient. Before the deposition, the Si substrate was primarily cleaned using a soap bath process to remove organic contaminants. The substrates were immersed in the cleaning solution at 60°C for 15 minutes, followed by an ultrasonic cleaning process to enhance the cleaning efficiency. After the soap bath, the substrates were rinsed sequentially with IPA and DI water to remove any residual contaminants. Finally, the substrates were dried with a nitrogen blow dryer. The sputtering conditions for the compositionally graded Al-Mo thin films were as follows: RF power of 75 W (Al) and 175 W (Mo), base pressure of 3.1×10^{-6} Pa, working pressure of 0.21 Pa, flow gas of Ar (99.99%), and room temperature substrate. The Al-Mo thin films were subsequently cut into 5 pieces, and the structural, chemical, and electrical properties of each sample were evaluated. Five Al-Mo samples with compositional gradients were named AM1 to AM5. The AM1 film refers to the Al-rich Al-Mo film grown near the Al target, while AM5 refers to the Mo-rich Al-Mo film grown near the Mo target. Three types of Al-Mo thin films with the uniform composition were deposited on 4-inch Si substrates through rotational growth. The sputtering conditions for these films were: RF power of 75 W (Al) and 75, 150, 300 W (Mo), base pressure of 3.1×10^{-6} Pa, working pressure of 0.21 Pa, flow gas of Ar (99.99%), and room temperature substrate. Three Al-Mo samples with uniform composition were named AM-a, AM-b, and AM-c, and these films were used to form the IDT electrodes for three types of SAW devices. The SAW-IDT pattern with a straight configuration was designed to have a resonant frequency of 143 MHz. This pattern consisted of the Al-Mo thin film thickness of 150 nm, a pattern width of 7 μm, a total IDT length of 3,000 μm, and 87 electrode pairs. The IDT electrode was patterned onto a 4-inch diameter $LiNbO_3$ (LN) substrate with a crystal orientation rotated 128 degrees from the +y axis through the +z axis about the x axis. Before depositing the IDT electrodes, the LN wafer was cleaned using Piranha solution, and then IDT patterns were formed using photolithography with a positive photoresist (AZ GXR 601). The Al-Mo thin films were deposited on the LN substrate using RF magnetron sputtering.

The compositional distribution and morphological properties of the Al-Mo thin films were examined by field emission scanning electron microscopy (FE-SEM, Quanta 200) with energy dispersive X-ray spectroscopy (EDS). The mixed density of the Al-Mo thin films was calculated based on the theoretical densities of Al and Mo elements according to the composition ratio of each film. Electrical resistivity was determined using the Hall Effect Measurement System with van der Pauw geometry (Model 7707, Lake Shore Cryotronics) at a constant magnetic field of 4 kG. The resistivity of the five Al-Mo thin films exhibiting compositional gradients was determined by taking the average of three repeated measurements. For the three Al-Mo thin films with uniform composition, the resistivity was obtained by averaging the results from three different samples. The IDT patterns were

observed using a 3D laser optical microscope (Model OLS4100-SAA, OLYMPUS). The resonant frequency of the SAW device was analyzed using a Vector Network Analyzer (Model E5080B, Keysight).

3. RESULTS AND DISCUSSION

Al-Mo thin films with compositional gradients were fabricated using combinatorial RF magnetron sputtering. As illustrated in Fig. 1, this technique enables the creation of a compositional gradient across the substrate, resulting in a sample library (AM1 to AM5) with continuously varying Al and Mo concentrations. The composition of each sample is directly correlated to its position on the substrate, allowing for a systematic study of the effects of composition on material properties while maintaining a constant film thickness. This approach enables accurate evaluation of the influence of compositional variations on material properties and contributes to the development of thin films with optimized compositions.

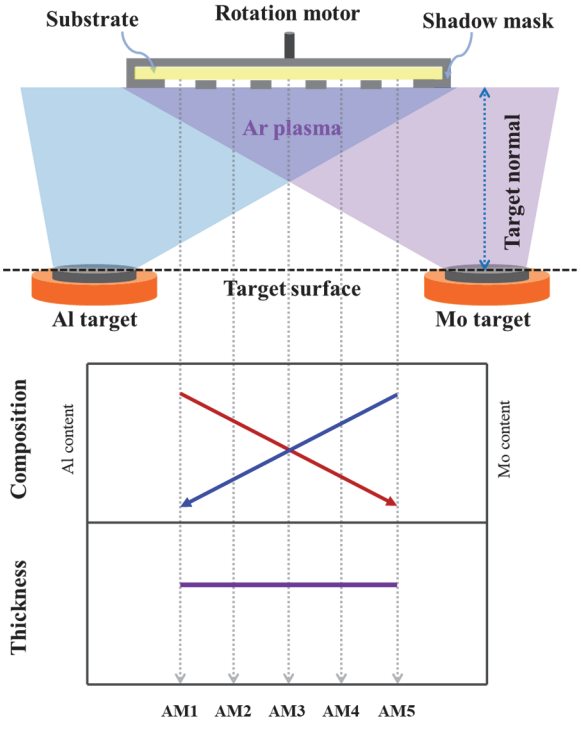

Fig. 1. Schematic diagram of combinatorial sputtering system to obtain the Al-Mo thin films with compositional gradients.

The AM1 thin film was located near the Al target, whereas the AM5 thin film was located near the Mo target. The Al-Mo thin films showed excellent adhesion to the substrate regardless of the sample position, and no defects, such as voids or cracks, were observed at the interface between the film and substrate. As shown in Fig. 2, all the Al-Mo thin films were grown to a constant film thickness, indicating that the Al-Mo thin films were distributed with a thickness of approximately 150 nm, regardless of the sample position. However, the compositions of the Al-Mo thin films intersect almost linearly with the sample position, and each sample has different Al and Mo contents. As the number of samples increased, the Al

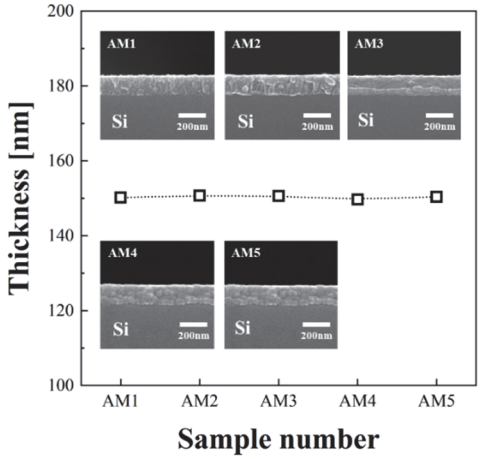

Fig. 2. Thickness distribution and cross-sectional SEM images of Al-Mo thin films deposited at different sample positions.

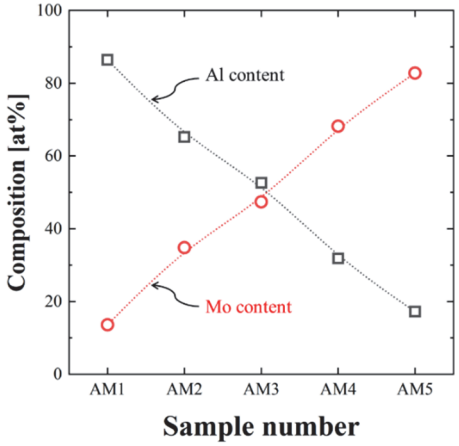

Fig. 3. Compositional variation of Al-Mo thin films as a function of sample number.

content decreased from 86.4 to 17.2 at% and the Mo content increased from 13.6 to 82.8 at%, as shown in Fig. 3.

Figure 4 shows the resistivity and calculated density of the Al-Mo thin films as functions of Al content. The resistivity of the Al-Mo thin films was distributed from 5.2±0.1 to 6.6±0.1×10^{-5} Ω-cm as the sample number increased, without a significant change. On the other hand, the calculated density changed significantly from 3.7 to 8.9 g/cm^3 as the sample number increased. The mixed densities of the Al-Mo thin films were calculated using the following simple equation:

$$\rho_{(Al\text{-}Mo)} = (\rho_{Al} \times V_{Al} + \rho_{Mo} \times V_{Mo}) / 100 \quad (1)$$

where ρ represents the theoretical density, and V represents the volume percentage. The densities of the Al-Mo mixed thin films were calculated by converting the atomic percentages of the five Al-Mo samples with varying Al and Mo contents to volume percentages. As shown in Fig. 3, the compositions of the Al-Mo thin films with the same thickness were linearly distributed according to the sample position. As the Al content in Al-Mo thin films with a constant thickness decreased, the electrical resistivity increased slightly, while the calculated density increased significantly. Given that these films were grown at room temperature, it is reasonable to assume that alloying did not occur. Consequently, in these physically mixed Al-Mo thin films, the electrical resistivity decreased as the content of Al, which has the lower resistivity compared to the Mo element, increased. Based on these results, the effect of the density of the Al-Mo IDT electrodes with the same film thickness and resistivity on the acoustic characteristics of the SAW device was investigated.

Through combinatorial studies, it was confirmed that the electrical and mechanical properties of the Al-Mo thin films vary with the Al content at the same film thickness. To form the SAW-IDT electrode, Al-Mo thin films with uniform composition should be prepared over the entire substrate. Therefore, three different types of compositionally uniform Al-Mo thin films were sputtered via rotational growth. Figure 5 shows the cross-sectional morphology of the three types of Al-Mo thin films grown on the Si substrate. The three types of Al-Mo thin films had an average film thickness of 150 nm, and no structural defects, such as voids or cracks, were observed between the substrate and the film. Table 1 presents the calculated density and resistivity of three Al-Mo thin films

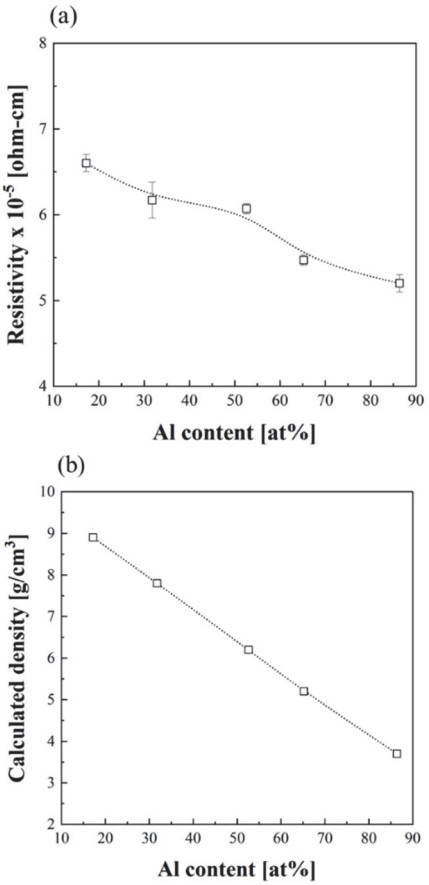

Fig. 4. Variations in resistivity (a) and calculated density (b) of Al-Mo thin films as a function of Al content.

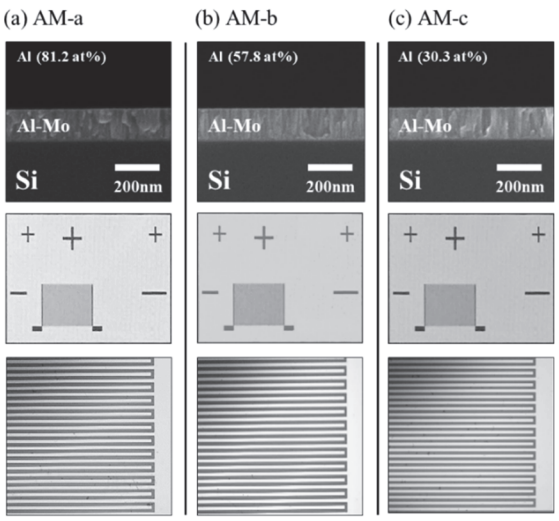

Fig. 5. SEM images of three Al-Mo thin films with uniform composition and optical microscope images of the corresponding SAW devices.

Table 1. Calculated density and resistivity of Al-Mo thin films as a function Al content.

Sample	Al content (at%)	Density (g/cm^3)	Resistivity (ohm-cm)
AM-a	81.2	4.1	$5.43\pm0.15\times10^{-5}$
AM-b	57.8	5.8	$5.47\pm0.15\times10^{-5}$
AM-c	30.3	7.9	$4.87\pm0.1\times10^{-5}$

with varying Al content, deposited on Si substrates via rotational growth. As the Al content increases from 30.3 at% (AM-c) to 81.2 at% (AM-a), the calculated density decreases from 7.9 g/cm^3 to 4.1 g/cm^3, respectively. This trend is consistent with the lower density of pure Al (2.7 g/cm^3) compared to pure Mo (10.2 g/cm^3).

Intriguingly, the resistivity of the Al-Mo films exhibits the less pronounced dependence on Al content than anticipated. While the general trend of increasing resistivity with decreasing Al content is observed, the magnitude of this variation is relatively small. For instance, the resistivity of AM-a (81.2 at% Al) is $5.43\pm0.15\times10^{-5}$ Ω-cm, while that of AM-c (30.3 at% Al) is $4.87\pm0.1\times10^{-5}$ Ω-cm. This suggests that factors beyond compositional differences may be influencing the electrical properties of these films. The relatively uniform resistivity among the Al-Mo samples can be attributed to the similar growth conditions and resulting microstructure. While various sputtering parameters, such as RF power, working pressure, deposition temperature, and film thickness, can significantly affect the resistivity of Al-Mo thin films, the primary variable in this study was RF power to achieve compositional grading. While RF power can influence the microstructure by altering the kinetic energy of sputtered atoms, it also affects the sputtering yield. Given the similar growth conditions and resulting microstructure of AM-a, AM-b, and AM-c, it is reasonable to expect a relatively small variation in resistivity as a function of composition in these physically mixed Al-Mo thin films. Consequently, IDT electrodes fabricated from Al-Mo thin films exhibiting comparable resistivities but significantly distinct densities will be employed to meticulously investigate the influence of these disparities on the resonant characteristics of SAW devices, including resonant frequency, insertion loss, and FWHM of the main frequency.

The SAW-IDT pattern composed of three kinds of Al-Mo thin films (AM-a, AM-b, AM-c) is designed to leverage acoustic radiation force for the manipulation of microparticles, specifically targeting the precise control of 5-micrometer (μm) polystyrene particles within a fluid medium. To obtain the resonant frequency suitable for the separation of 5 μm PS particles, the acoustic frequency was calculated using the following equation [10]:

$$f = c_s / \lambda \quad (2)$$

where c_s is the speed of acoustic waves in the piezoelectric substrate, and λ is the wavelength of SAWs. The wavelength of the SAWs is dependent on the structure of the IDTs, which can be calculated as [10]

$$\lambda = 4d \quad (3)$$

where λ is the wavelength of the SAWs, and d is the width of the IDTs (assuming the width and spatial distance of the IDTs are the same).

Based on the above relationships, the correlation between the IDT pattern width, the number of IDT electrodes, film thickness, and total electrode length was clarified using Mathematica, and the influence on the intensity and frequency of the acoustic waves generated from the SAW device was investigated. The resonant frequency corresponding to the IDT pattern width was analyzed using the above equation, and the SAW-IDT pattern width of 7 μm is required to achieve a resonant frequency of 143 MHz. In addition, 87 IDT electrode pairs and the total IDT length of 3,000 μm were selected to satisfy the reference impedance of 50 Ω.

Figure 6 shows the resonant frequencies fabricated with the Al-Mo thin films with different Al contents of 81.2 (sample number: AM-a), 57.8 (sample number: AM-b), and 30.3 (sample number: AM-c) at%. All three types of SAW devices have the same pattern width of 7 μm, total IDT length of 3,000 μm, film thickness of 150 nm, and 87 electrode pairs. All the three SAW devices exhibited the same resonant frequency of approximately 143 MHz, confirming that they were fabricated normally without defects in the designed IDT patterns. As the Al content of the IDT electrode composed of Al-Mo thin films decreased, the insertion loss at the resonant frequency decreased rapidly from -9.3 to -3.4 dB, and the FWHM of the main frequency gradually increased from 1.6 to 3.4 MHz. These findings indicate that the resonant characteristics of the SAW devices fabricated with Al-Mo thin films were more

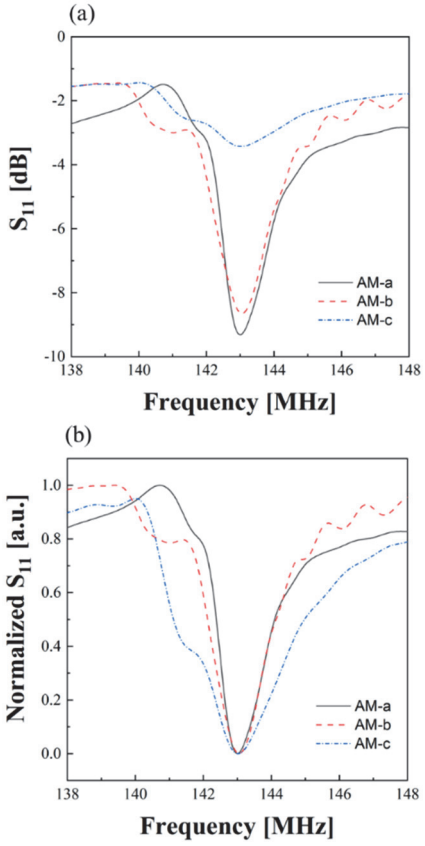

Fig. 6. Resonant frequency characteristics (a) and normalized curves (b) of SAW devices fabricated using three types of Al-Mo thin films.

strongly influenced by the material density rather than the electrical properties of the IDT electrodes. The density of IDTs fabricated on the piezoelectric substrate significantly influences the efficiency of lattice vibrations induced in the piezoelectric material during the conversion of electrical energy to mechanical energy via the inverse piezoelectric effect. When an external electric field is applied to the piezoelectric material, its crystal structure undergoes deformation, generating mechanical vibrations. A lower IDT density can lead to more efficient lattice vibrations in the piezoelectric material, thus enhancing acoustic performance. In addition, While the electrical resistivity of Al-Mo thin films decreased by approximately 18% with decreasing Al content, the material density exhibited a substantial increase of approximately 240%. As previously discussed, the relatively small variation in electrical resistivity, despite the significant change in Al content, can be attributed to the similar crystal structures of the three Al-Mo thin films and the relatively small difference in resistivity between pure Al and Mo. Consequently, among the three samples, the SAW device composed of the Al-rich AM-a thin film demonstrated the best performance.

4. CONCLUSION

This study investigated the influence of Al content on the resonant characteristics of Al-Mo thin film-based Surface Acoustic Wave (SAW) devices. A combinatorial approach was employed to explore the structural, electrical, and mechanical properties of Al-Mo thin films as a function of composition. Three Al-Mo thin films with uniform compositions were selected as SAW-IDT electrode materials to examine their impact on the acoustic characteristics of SAW devices. The SAW devices fabricated with Al-Mo thin films exhibited a decrease in insertion loss and an increase in quality factor as the Al content decreased. These findings suggest that the material density of the Al-Mo thin films plays a more dominant role in determining the resonant characteristics than the electrical properties. Our results highlight the potential for optimizing Al content in Al-Mo thin films to enhance SAW device performance. By increasing Al content, it is possible to achieve lower insertion loss and narrower bandwidth, leading to improved sensitivity and selectivity in SAW sensors. Future studies could explore the effects of other material properties, such as grain size and film morphology, on the resonant characteristics of Al-Mo based SAW devices. In conclusion, this research provides valuable insights into the relationship between Al content and the resonant characteristics of Al-Mo thin film-based SAW devices.

ORCID
Jae-Cheol Park https://orcid.org/0000-0003-3615-3933

ACKNOWLEDGMENT

This research was financially supported by the Ministry of Small and Medium-sized Enterprises(SMEs) and Startups (MSS), Korea, under the “Regional Specialized Industry Development Plus Program(R&D, S3401805)” supervised by

the Korea Technology and Information Promotion Agency(TIPA) for SMEs. In addition, this study was conducted with the support of the Korea Industrial Complex Corporation as a 'Competitiveness reinforcement project for industrial clusters (1415189052)'.

REFERENCES

[1] K. Länge, B. E. Rapp, and M. Rapp, *Anal. Bioanal. Chem.*, **391**, 1509 (2008).
doi: https://doi.org/10.1007/s00216-008-1911-5

[2] S. Qureshi, M. Hanif, V. Jeoti, G. M. Stojanović, and M. T. Khan, *Results Eng.*, **22**, 102323 (2024).
doi: https://doi.org/10.1016/j.rineng.2024.102323

[3] C. Wang, Y. Ding, M. Li, H. Li, S. Xu, C. Li, L. Qian, and B. Yang, *Anal. Chim. Acta*, **1190**, 339264 (2022).
doi: https://doi.org/10.1016/j.aca.2021.339264

[4] Z. Jiang, B. Liu, L. Yu, Y. Tong, M. Yan, R. Zhang, W. Han, Y. Hao, L. Shangguan, S. Zhang, and W. Li, *J. Alloys Compd.*, **956**, 170316 (2023).
doi: https://doi.org/10.1016/j.jallcom.2023.170316

[5] R. Augustine, F. Sarry, N. Kalarikkal, S. Thomas, L. Badie, and D. Rouxel, *Nano-Micro Lett.*, **8**, 282 (2016).
doi: https://doi.org/10.1007/s40820-016-0088-2

[6] P. Rajput, J. Kumar, U. Mittal, A. T. Nimal, A. V. Arsenin, V. S. Volkov, and P. Mishra, *Inorg. Chem. Commun.*, **146**, 110116 (2022).
doi: https://doi.org/10.1016/j.inoche.2022.110116

[7] E. Unosson, D. Rodriguez, K. Welch, and H. Engqvist, *Acta Biomater.*, **11**, 503 (2015).
doi: https://doi.org/10.1016/j.actbio.2014.09.048

[8] A. Jabed, M. M. Khan, J. Camiller, M. Greenlee-Wacker, W. Haider, and I. Shabib, *Surf. Coat. Technol.*, **372**, 278 (2019).
doi: https://doi.org/10.1016/j.surfcoat.2019.05.036

[9] H. N. Barad, M. Alarcón-Correa, G. Salinas, E. Oren, F. Peter, A. Kuhn, and P. Fischer, *Mater. Today*, **50**, 89 (2021).
doi: https://doi.org/10.1016/j.mattod.2021.06.001

[10] X. Liu, X. Chen, Z. Yang, H. Xia, C. Zhang, and X. Wei, *Sens. Diagn.*, **2**, 507 (2023).
doi: https://doi.org/10.1039/D2SD00203E